Lattice Boltzmann simulation of solute transport in heterogeneous porous media with conduits to estimate macroscopic continuous time random walk model parameters

Shadab Anwar

Department of Earth Sciences,
Florida International University,
University Park, Miami, FL 33199, USA
E-mail: sanwa001@fiu.edu

Andrea Cortis

Earth Sciences Division,
Lawrence Berkeley National Laboratory,
1 Cyclotron Road Berkeley, CA 94720, USA
E-mail: acortis@lbl.gov

Michael C. Sukop*

Department of Earth Sciences,
Florida International University,
University Park, Miami, FL 33199, USA
E-mail: sukopm@fiu.edu
*Corresponding author

Abstract: Lattice Boltzmann models simulate solute transport in porous media traversed by conduits. Resulting solute breakthrough curves are fitted with Continuous Time Random Walk models. Porous media are simulated by damping flow inertia and, when the damping is large enough, a Darcy's Law solution instead of the Navier-Stokes solution normally provided by the lattice Boltzmann model is obtained. Anisotropic dispersion is incorporated using a direction-dependent relaxation time. Our particular interest is to simulate transport processes outside the applicability of the standard Advection-Dispersion Equation (ADE) including eddy mixing in conduits. The ADE fails to adequately fit any of these breakthrough curves.

Keywords: porous media; solute transport; lattice Boltzmann; CTRW.

Reference to this paper should be made as follows: Anwar, S., Cortis, A. and Sukop, M.C. (2008) 'Lattice Boltzmann simulation of solute transport in heterogeneous porous media with conduits to estimate macroscopic continuous time random walk parameters', *Progress in Computational Fluid Dynamics*, Vol. 8, Nos. 1–4, pp.213–221.

Biographical notes: Shadab Anwar is a PhD student in the Department of Earth Sciences at Florida International University. His research interests include environmental engineering applications of Lattice Boltzmann Methods–especially solute transport in complex porous media.

Andrea Cortis is Geological Scientist in the Earth Sciences Division of the Lawrence Berkeley National Laboratory. His research interests include: transport of mass, momentum and energy in multiple-scale heterogeneous media; porous media upscaling theories; soft computing optimisation methods; deterministic fractal-multifractal data representation; nano-materials for groundwater remediation.

Michael Sukop is Assistant Professor of Earth sciences at Florida International University where he conducts research on applications of Lattice Boltzmann Methods to Earth and environmental science.

1 Introduction

Solute transport through heterogeneous porous media has generally been represented by Fickian advection dispersion models. Several analytical and numerical models have been proposed and applied in the past. Such traditional models cannot predict the anomalous behaviors like sudden breakthrough and long tailing that are expected in porous media traversed by conduits.

The Continuous Time Random Walk (CTRW) model can be used to simulate solute transport under complex conditions. This method is based upon a probability distribution function (pdf) that defines the transition time of solute particles and ultimately depends upon the hydrological and geological parameters. CTRW has been found successful in modelling non-Fickian transport in heterogeneous porous media (Cortis and Berkowitz, 2004).

Solute transport through porous media has been widely studied at various scales and the ADE is generally used as the tool for quantifying and predicting solute transport. The basic assumption of the ADE is that dispersion follows Fickian behaviour and hence breakthrough curves of pulse inputs follow a Gaussian distribution (Berkowitz et al., 2006).

Numerous experiments have shown that solute spreading does not follow a Gaussian distribution. The main reason for this non-Fickian behavior of solute transport in porous media is the presence of heterogeneity in medium properties like porosity, permeability, etc., at various scales. The variations in medium properties affect the velocity of and path traveled by solute particles and consequently the time of travel varies with heterogeneity of the medium.

1.1 AADE

The traditional governing equation for mass transport of a solute subjected to advection and anisotropic dispersion in porous media is a partial differential equation called the Anisotropic Advection-Dispersion Equation (AADE), which in a 2D Cartesian formulation reads

$$\frac{\partial C}{\partial t} + \overline{U}_x \frac{\partial C}{\partial x} = \frac{\partial}{\partial x}\left(D_{xx}\frac{\partial C}{\partial x}\right) + \frac{\partial}{\partial y}\left(D_{yy}\frac{\partial C}{\partial y}\right), \quad (1)$$

where C is solute concentration (ML^{-3}), $\overline{U}_x$ is the mean velocity in the X-direction (LT^{-1}), D_{ij} is the diffusion/dispersion coefficient (L^2T^{-1}) in the ij direction, x and y are spatial coordinates (L) and t is time (T). Equation (1) is the governing equation for mass transport in two dimensions under the assumption of Fickian dispersion, when macroscopic flow is in the x-direction. The second term on the LHS of Equation (1) represents the rate of mass transport due to advection alone and terms on the right hand side represent mass transport due to dispersion, which depends upon the dispersion coefficients (dispersion tensor) D_{xx} and D_{yy} in respective directions. Longitudinal (D_{xx}) and transverse (D_{yy}) dispersion coefficients account for anisotropic dispersion in porous media.

Advection, mechanical dispersion, and diffusion are the dominant mechanisms for transport of solute in porous media. When advection is significant, dispersion is unequal between the longitudinal and transverse directions, but when the advection rate is small and diffusion is dominant, the longitudinal (D_{xx}) and transverse (D_{yy}) dispersion coefficients are nearly equal (Freeze and Cherry, 1979). The process of mechanical dispersion is anisotropic even if the porous medium is isotropic with respect to pore orientation and hydraulic conductivity because flow in the longitudinal direction aligned with the mean velocity is dominant and that stretches the solute plume into an elliptical shape (Freeze and Cherry, 1979). Hence anisotropic dispersion must be considered if simulation is performed at Darcy scale where detailed within-pore flows are not resolved.

Porous media, in general, can exhibit multiple scale heterogeneity and transport parameters must be linked properly at various scales for accurate solute transport modelling. In the past, several models have been proposed for porous media traversed by conduits in which the domain is divided into zones and different analytical models like the Darcy-Weisbach equation, Poiseuille (cubic) law, and Darcy's law are used for flux calculation as appropriate in different zones (Field, 1993; White and White, 2005). These models may be applicable for Stokes flow in geometrically simple domains, but in transition and turbulent regimes and complex domains, such models may not be appropriate.

2 LBM

2.1 Flow model

The standard Bhatnagar-Gross-Krook (BGK) collision-based D2Q9 (2-dimensional, 9 velocity) model (Qian et al., 1992) is used to simulate fluid flow in open channels in this work. The macroscopic fluid density (ρ) for the model is

$$\rho = \sum_{j=0}^{8} f_j. \quad (2)$$

The macroscopic velocity $\mathbf{u}$ is an average of the microscopic velocities $\mathbf{e}_j$ weighted by the directional densities f_j:

$$\mathbf{u} = \frac{1}{\rho}\sum_{j=0}^{8} f_j \cdot \mathbf{e}_j \quad (3)$$

where $[\mathbf{e}_0 \ \mathbf{e}_1 \ \mathbf{e}_2 \ \mathbf{e}_3 \ \mathbf{e}_4 \ \mathbf{e}_5 \ \mathbf{e}_6 \ \mathbf{e}_7 \ \mathbf{e}_8] =$

$$\begin{bmatrix} 0 & 1 & 0 & -1 & 0 & 1 & -1 & -1 & 1 \\ 0 & 0 & 1 & 0 & -1 & 1 & 1 & -1 & -1 \end{bmatrix} c$$

and c is the unit speed on the lattice, 1 lattice unit per time step.

Equations (2) and (3) link the mesoscopic particle distribution with the macroscopic density and velocity of the fluid.

Key steps are streaming and collision of the particles via the distribution function. The simplest approach uses the BGK approximation for collision as described below.

Equation (4) represents the time evolution of the Particle Distribution Function (PDF) (Qian et al., 1992):

$$f_j(\mathbf{x}+\mathbf{e}_j\delta t, t+\delta t) = f_j(\mathbf{x},t) - \delta t\left(\frac{f_j(\mathbf{x},t)-f_j^{eq}(\mathbf{x},t)}{\tau}\right), \quad (4)$$

where $f_j(\mathbf{x}+\mathbf{e}_j\delta t, t+\delta t) = f_j(\mathbf{x},t)$ is the streaming part and $\delta t\left(\frac{f_j(\mathbf{x},t)-f_j^{eq}(\mathbf{x},t)}{\tau}\right)$ is the collision term representing the rate of change of the particle distribution function due to collision. The collision operator is simplified in the BGK model by use of a single relaxation time τ for all directions. τ is a relaxation time that indicates the rate at which the system approaches equilibrium through collision. The equilibrium distribution function f^{eq} is (Qian et al., 1992)

$$f_j^{eq}(\mathbf{x}) = t_j^*\rho(\mathbf{x})\left(c_s^2 + \mathbf{e}_j\cdot\mathbf{u} + \frac{3}{2}(\mathbf{e}_j\cdot\mathbf{u})^2 - \frac{1}{2}\mathbf{u}^2\right), \quad (5)$$

where c_s is the speed of sound, a free parameter in Equation (5). $c_s^2 = \frac{1}{3}$ in the present study. The weights (t_j^*) are $\frac{1}{3}$ for $j = 1,2,3,4$ (main Cartesian axes), and $\frac{1}{12}$ for $j = 5,6,7,8$ (diagonals). The weight for $j = 0$ rest particles is $t_0 = 1 - c_s^2\sum t_j = 1 - \frac{5}{3}c_s^2 = \frac{4}{9}$ (Ginzburg, 2005). Note that if $\mathbf{u} = 0$, the equilibrium distribution function elements f_j^{eq} are simply the weights times the fluid density.

For the simulations we present below, we apply either periodic or pressure boundary conditions for the fluid flow. For the pressure boundaries, we adopt the methods of Zou and He (1997) in which incoming fs are computed based on the desired pressure and the known fs. In contrast to the bounce-back boundaries discussed below, the pressure boundaries are applied at the actual locations of the nodes.

2.2 *Solute transport model*

Flekkøy (1993) introduced an LB model to simulate diffusion of miscible fluid flow in 2D and 3D. A separate equilibrium distribution function with its own relaxation parameter is derived to simulate the advection-diffusion equation. Equilibrium distribution functions for flow and transport are coupled with a common macroscopic flow velocity; hence the solute component behaves as a passive scalar.

In this approach two components A and B are assumed and one is a very small fraction of the other, therefore collisions between A-B or B-A are assumed negligible and not included in the computation (Inamuro et al., 2002). Component A will have the same equilibrium function as the regular BGK LB model (i.e., it will behave as a regular fluid) but component B will evolve towards a new equilibrium as expressed by its own equilibrium distribution function, which unlike Equation (4) for component A, contains only the terms up to first order in flow velocity, as shown in Equation (6) (Flekkøy, 1993):

$$f_{Bj}^{eq}(\mathbf{x}) = t^*\rho_B(\mathbf{x})[c_s^2 + \mathbf{e}_j\cdot\mathbf{u}_A]. \quad (6)$$

The density (concentration) for component B is computed following Equation (2) and its velocity $\mathbf{u}_A$ is assigned from component A; B is advected as a passive scalar. The mass diffusivity D_m between two species is expressed in terms of relaxation time τ_B for component B (Flekkøy, 1993):

$$D_m = c_s^2\left[\tau_B - \frac{1}{2}\right]. \quad (7)$$

LBM is not free from numerical diffusion. We estimated numerical diffusion at a moving solute front. At a velocity of 0.01 lu/ts and an expected diffusion of $3.33\bar{3}\times 10^{-3} lu^2/ts$, we found that the observed diffusion coefficient was on the order of $10^{-5} lu^2/ts$ greater (approximately 1% greater). The diffusion coefficient was approximately 3% higher at a velocity of 0.05 lu/ts, which is the same as the highest velocity in our results section. See Ginzburg (2005) for an improved equilibrium function that reduces numerical diffusion for certain LBM transport models.

Two types of boundary conditions are applied to the solute; the first is constant concentration and the second is zero concentration gradient, which allows advective flux but prohibits diffusive and dispersive fluxes. Much like the Zou and He (1997) boundaries applied to the flow, the constant concentration boundary is based on ensuring that the sum of the unknown incoming fs plus the known fs equal the desired concentration (Inamuro et al., 2002). The zero concentration gradient boundary requires that the solute fs on each side of the boundary node are balanced; Sukop and Thorne (2006) contains more detailed descriptions of these boundaries.

2.3 *Macroscopic porous media approach*

Fluids flowing through porous media experience resistance that depends in part on the volume density of solids (the porosity) because no-slip conditions at fluid-solid interfaces resist the flow and generally become dominant as the porosity decreases. When this resistance is large enough relative to driving forces, flow is non-inertial and governed by Darcy's law. At higher porosity, in larger conduits, or under high driving force, resistance is lower and flows transition towards free fluid flows governed by the Navier-Stokes equation as the Reynolds number increases and inertial components of the flow become more important. Partial damping of inertial components that allows simulation of a continuum of flows from strictly non-inertial, Darcy's law behaviour, through transitional and inertially-dominated flows at higher Reynolds numbers can be considered an advantage. It may reflect the behavior of real porous media better than a strict Darcy's law/Stokesian solution when the permeability is especially high and/or when gradients are high enough that inertial effects can be important. Several models have been proposed to model flow in heterogeneous porous media (Balasubramaniyam et al., 1987; Gao and Sharma, 1994; Spaid and Phelan, 1997; Dardis and McCloskey, 1998; Kang et al., 2002; Freed, 1998) and usually use either a damping factor or force that

allows this Darcy-to-inertial transition. When appropriate, it is also possible to exclude the potential for inertial components in porous medium flow by truncating the inertial terms that appear in the equilibrium distribution function, Equation (5).

Balasubramaniyam et al. (1987) introduced a velocity-dependent damping term in the Navier-Stokes equations to approximate Darcy's law in porous media at macroscopic scale in a hexagonal lattice, lattice gas model context. The approach we implement here is based on Balasubramaniyam et al. (1987) extended to hexagonal lattice Boltzmann models by Dardis and McCloskey (1998), but numerous other approaches are available. The modified N-S equation with damping term βu is

$$\nu \frac{d^2 u}{dx^2} - \beta u = \frac{1}{\rho} \frac{dp}{dy}, \tag{8}$$

where, β is linked with a scatterer density n_s, which can be viewed as loosely related to the porosity of a medium (Balasubramaniyam et al., 1987). The relationship is $\beta = 2n_s$ (Balasubramaniyam et al., 1987). Gao and Sharma (1994) has defined n_s either as a fraction of solid nodes in the porous medium or probability of each node being a solid, but interpreting it as simply a damping factor inversely proportional to permeability over certain ranges may be most appropriate. In this case, there are no distinct pores and solids and the kinematic viscosity ν no longer retains its normal meaning but instead, along with n_s, determines k in lattice units according to $k = \frac{\nu}{2n_s}$. We always use a single kinematic viscosity throughout the domain and use n_s alone to vary k.

This model can simulate at large (Darcy) scale without incurring the excessive computational requirements characteristic of pore scale modelling. To implement the LBM for macroscopic porous media, there is an additional collision step after streaming and BGK collision. Denote the PDFs after standard BGK collision by

$$f_j^{**}(\mathbf{x}, t+\delta t) = f_j^{*}(\mathbf{x}, t) + \frac{f_j^{eq}(\mathbf{x}, t) - f_j^{*}(\mathbf{x}, t)}{\tau} \tag{9}$$

where f^* denotes the PDFs after streaming. Then the porous media step is implemented as an additional term involving the f^{**}

$$f_j(\mathbf{x}, t+\delta t) = f_j^{**}(\mathbf{x}, t+\delta t) + n_s(\mathbf{x})\left[f_{j+2}^{**}(\mathbf{x} + \mathbf{e}_j \delta t, t+\delta t) - f_j^{**}(\mathbf{x}, t+\delta t)\right]. \tag{10}$$

This reduces to standard BGK collision when $n_s = 0$. For values of n_s between 0 and 1, we have a partial bounce-back like condition that makes the medium effectively porous; i.e., the flow can be described by Darcy's law. We can have a different n_s value at each node in the domain. Depending upon the scale, each node could represent a large homogeneous domain.

The effective permeability is given approximately by $k = \frac{\nu}{\beta}$ for $n_s < 0.5$. In Sukop and Thorne (2006), simulations with the same code as that applied in this study show reasonable agreement with $k = \frac{\nu}{2n_s}$, but no formal error analysis is available at this time. Moreover, a number of other methods (e.g., Spaid and Phelan, 1997; Kang et al., 2002; Freed, 1998; Capuani et al., 2003) have been proposed and may be superior to what we apply in this work. The emphasis here is on demonstrating the ability to account for relative permeability differences via the damping factor and superimpose anisotropic solute transport; additional work is needed to quantify the accuracy of the method.

Drawbacks of the lattice BGK equation with the bounce-back boundary conditions have become evident during permeability calculations in pore-scale porous media simulations (Pan et al., 2006). It has been shown (Ginzburg and d'Humières, 2003; Pan et al., 2006) that the inaccuracy observed in the BGK model can be effectively removed by using the Multiple-Relaxation-Time (MRT) models, or in the case of the standard BGK model, by setting the relaxation parameter (τ) equal to 1 and assuming the effective wall position to be located about halfway between the fluid and solid nodes. Of the simulations presented in this paper, all but two have $\tau = 1$. In the first high Re (low τ, Fig. 6) case, our simulation suffers from a relatively small error in wall location. In the second case (Fig. 9) – where we use the damping factor to simulate the permeable walls of a channel – strict bounce-back is not being applied and no analysis of potential inaccuracies is available to the best of our knowledge.

2.4 *Anisotropic LBM*

The BGK model is the simplest form of collision mechanism in the LB equation and has a single lumped relaxation time for each direction that gives isotropic diffusion when the passive scalar approach is applied. This is appropriate for the simulation of diffusion in free flowing fluids. However as explained above, in the solute transport process in porous media when the flow is not negligible, dispersion is inherently anisotropic; thus, an anisotropic dispersion solver is needed to develop an LB model with capabilities comparable to those of standard porous media solute transport solvers. The dispersion coefficients in Equation (1) are found using the following equation (Bear, 1979):

$$D_{ij} = \alpha_T \sqrt{u_x^2 + u_y^2}\,\delta_{ij} + \frac{(\alpha_L - \alpha_T) u_i u_j}{\sqrt{u_x^2 + u_y^2}} \tag{11}$$

where, δ_{ij} is Kronecker delta, α_L and α_T are dispersivity coefficients in the longitudinal and transverse directions respectively. i and j represent the Cartesian directions (x or y). For heterogeneous domains, velocity (u_x, u_y) changes at every node, so the dispersion coefficient does too.

Zhang et al. (2002a) and Ginzburg (2005) introduced LB models with more than one relaxation parameter in the collision mechanism to simulate anisotropic dispersion. Zhang's approach (Zhang et al., 2002a, 2002b) appeared first in the literature and we implemented it before Ginzburg (2005) was published. Ginzburg's method (Ginzburg, 2005) is more rigorous. Zhang's method

(Zhang et al., 2002a) has four relaxation parameters in nine directions to simulate anisotropic dispersion. Conservation of mass is ensured by taking a weighted summation of the particle distribution function, so that the collision step remains mass invariant (Zhang et al., 2002a). The mass is calculated as (Zhang et al., 2002a)

$$m = \sum_j \frac{f_j}{\tau_j} \sum_j \left(\frac{t_j^* c_s^2}{\tau_j} \right)^{-1} \tag{12}$$

and the dispersion tensor in terms of relaxation parameters τ is expressed as:

$$\begin{aligned} D_{xx} &= \frac{\delta x^2}{18\delta t}[4\tau_1 + \tau_5 + \tau_8 - 3], \\ D_{yy} &= \frac{\delta y^2}{18\delta t}[4\tau_4 + \tau_5 + \tau_6 - 3], \\ D_{xy} &= \frac{\delta x \delta y}{18\delta t}[\tau_5 - \tau_6]. \end{aligned} \tag{13}$$

We use $\delta x = \delta y = 1$ and $\delta t = 1$.

Four relaxation parameters are back calculated from dispersion coefficients. It is obvious from Equation (13) that there is no one-to-one relation between relaxation parameters and dispersion coefficients. Hence one of the relaxation parameter is chosen and rest are calculated using Equation (13). The relaxation parameters are so chosen that they are close to each other but not too close to 0.5 to avoid numerical instability (Zhang et al., 2002b).

This will provide an LBM-based anisotropic dispersion solver comparable to those found in standard porous media solute transport models while the regular LB model with $\tau_s = 0$ retains the potential to solve the Navier-Stokes equation and the advection diffusion equation in conduits. This model is verified against one- and two-dimensional analytical solutions for various boundary conditions (Zhang et al., 2002a, 2002b).

3 CTRW

Unlike the ADE, the CTRW does not separate a priori between advective and dispersive components to keep track of the solute movement. For a detailed account of the CTRW method, we refer the reader to the recent review by Berkowitz et al. (2006). The initial conservation equation is the so-called Master equation,

$$\frac{\partial}{\partial t} C_i(t) = w_{ij} C_j(t), \tag{14}$$

where w_{ij} is the transition rate $[1/T]$ of C from point x_j to x_i, which describes the fine details of the microscopic heterogeneity. As a fully detailed deterministic description of the heterogeneity is impossible to achieve in practice, Equation (14) is ensemble averaged over all possible realisations of the heterogeneity to obtain

$$u\bar{C}_i(t) - C(t=0) = \widetilde{W}_{ij}(u)\bar{C}_j(u), \tag{15}$$

where the tilde $\bar{}$ indicates the Laplace transform $\bar{C}(u) \equiv \mathcal{L}[C(t);u] \equiv \int_0^\infty C(t)\exp(-ut)dt$, and u is the Laplace variable. The quantity $\widetilde{W}_{ij}(u)$ is intimately related to the waiting-time probability distribution function, $\Psi(x,t)$ of a *jump* of length x in the time interval t (Berkowitz et al., 2006). Introducing the decomposition $\Psi(x,t) = \psi(t)p(x)$, and assuming that $p(x)$ has finite first and second moment, it is possible to write the PDE that governs the solute transport in heterogeneous formations. The one dimensional form of this PDE reads

$$\begin{aligned} &u\bar{C}(x,u) - C_0(x) \\ &\quad = -\widetilde{M}(u)\bar{U}\frac{\partial}{\partial x}\left[\bar{c}(x,u) - \alpha\frac{\partial}{\partial x}\bar{c}(x,u)\right]. \end{aligned} \tag{16}$$

Equation (16) introduces a time convolution of the classical advection-dispersion spatial operator with a memory function, $\widetilde{M}(u)$, defined in terms of waiting time pdf $\psi(t)$

$$\widetilde{M}(u) \equiv \bar{t}u\frac{\bar{\psi}(u)}{1-\bar{\psi}(u)}, \tag{17}$$

and a characteristic time $\bar{t}$. The identification of the $\psi(t)$ rests at the heart of the CTRW method. Note that when $\psi(t) = \exp(-t)$, we have $\mathcal{L}[\exp(-t);u] = 1/(1+u)$, and thus $\widetilde{M}(u) = 1$; that is, the classical ADE is a special case of the CTRW transport equation. For any other shape of the probabilistic distribution, $\widetilde{M}(u) \neq 1$, and memory effects are manifest in the behavior of the solute. A host of parametric forms for $\psi(t)$ has been successfully used in the literature to fit experimental breakthrough curves and are described in detail in Berkowitz et al. (2006).

In this approach, the parameters of the $\psi(t)$ pdf augment the classical number of transport parameters in the 1-D advection dispersion equation (i.e., $\bar{U}_x$, and α) and a best fit to the data is sought on this parameter space.

This approach, however, fails to describe the more complex situations described in this work. In our search for a CTRW model, we therefore adopt a different point of view that consists in a numerical deconvolution of the full time evolution of $\psi(t)$ (Cortis, 2007). We want to analyse some breakthrough curve (BTC) $c_e(t)$ sampled at the section x_0 for discrete number of points t_j in the interval $\Delta t = [t_{\min}, t_{\max}]$. We evaluate an approximation of the Laplace transform (truncated over Δt) of the 'experimental' BTC $c_e(t)$ by means of a Clenshaw-Curtis quadrature algorithm for N Laplace variables $u_i \in \mathcal{C}$, $(i = 1 \ldots N)$. The values of u_i are dictated by the particular choice of the numerical algorithm for the Laplace transform inversion (Berkowitz et al., 2006).

We can now search for the real and imaginary values of $\bar{\psi}(u_i)$ that minimise the norm between $\bar{c}(u_i)$, the solution of Equation (16) at the given section x_0 (for a suitable set of boundary conditions), and $\bar{c}_e(u_i)$, the numerical Laplace transform of $c_e(t)$. This non-linear minimisation procedure is repeated for all values of u_i to obtain a numerical approximation of $\bar{\psi}(u_i)$.

Numerical inversion of $\bar{\psi}(u_i)$ finally yields the time evolution of $\psi(t)$. In order to perform the inversion procedure on the memory function we need, however, to fix the value of α. The dispersivity α is in general

not a datum of the problem and can only be given an a priori estimated value in some interval $[\alpha_{min}, \alpha_{max}]$, where $\alpha_{min} \sim D_{diff}$ the diffusion coefficient for the solute in the water, and $\alpha_{max} \sim d$, the characteristic length for the pore throat size. The non-parametric inversion of $\psi(t)$ yields thus a family of pdf's $\psi(t|\alpha)$ depending on the parameter α, and each member of the parametric family yields a best fit on the data, $c_e(t_j)$. The reason for this behavior is easily understood by considering that the CTRW PDE in Equation (16) decouples the effects of the spatial and temporal parts of the probability distribution of waiting times $\Psi(x,t)$ into two statistically independent distributions, $\Psi(x,t) \equiv p(x)\psi(t)$, defining thus a non-dimensional dispersivity (inverse of the Peclet number, $\alpha/L \equiv Pe^{-1}$)

$$\frac{\alpha}{L} = \frac{1}{2}\frac{\int p(x)x^2\,dx}{\int p(x)x\,dx} \tag{18}$$

where L is a characteristic macroscopic length scale. As the $p(x)$ distribution needs only to be characterised by its first two moments, the decomposition of $\Psi(x,t) = p(x)\psi(t)$, is not unique, hence the expression for the $\psi(t)$ is not unique. We note, however, that we can usually have very good fit of the BTC by imposing small values of α, i.e., by distributing the effect of the spreading more into the temporal part (the waiting time pdf $\psi(t)$) rather than the on the spatial component (the dispersivity). The consistency of the choice of the small scale Pe will ultimately be assessed only by looking at BTC predictions over different sections x, which we reserve for future work.

4 Results and discussion

The value of combining the CTRW and LBM approaches is that complete knowledge of the velocity field is available from the LBM simulations and domain heterogeneity can be varied at will. In the comparisons of CTRW and ADE models that follow, the CTRW is applied in a 1-D macroscopic fashion to the 2-D LBM simulations. That is, while the LBM solves the AADE described above, the macroscopic ADE and CTRW used to fit the results treats the flow and transport as macroscopically 1-D.

4.1 Poiseuille flow

One of the simplest types of breakthrough curves is that which corresponds to Poiseuille flow and solute transport without diffusion. This problem has an easily-derived analytical solution and can be closely approximated by LBM simulation. However, this breakthrough curve cannot be fitted with the ADE. We use a domain $1000\,lu \times 82\,lu$ to simulate solute transport with near-zero diffusion for periodic flow in a slit. The flow is gravity driven at $g = 6 \times 10^{-6} lu/ts^2$. Relaxation parameters τ for fluid and solute are $1.0\ ts$ and $0.501\ ts$ respectively. The average velocity of flow is $0.02\ lu/ts$.

Figure 1 shows the $\psi(t)$ function and Figure 2 shows the LBM simulation together with the best-fitting ADE and CTRW solutions. The CTRW is clearly capable of fitting this simple breakthrough curve.

Figure 1 ψ function against pore volume for zero diffusion transport between parallel plates

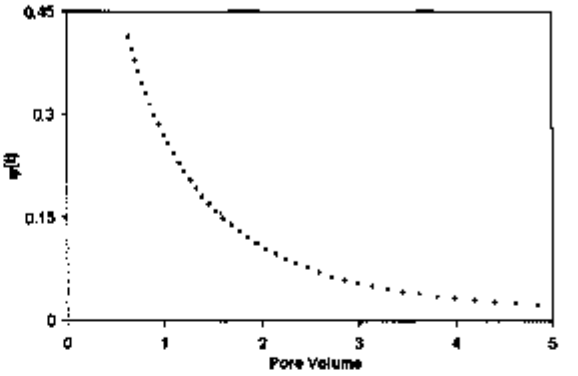

Figure 2 Zero diffusion breakthrough curve from LBM fitted with CTRW and ADE

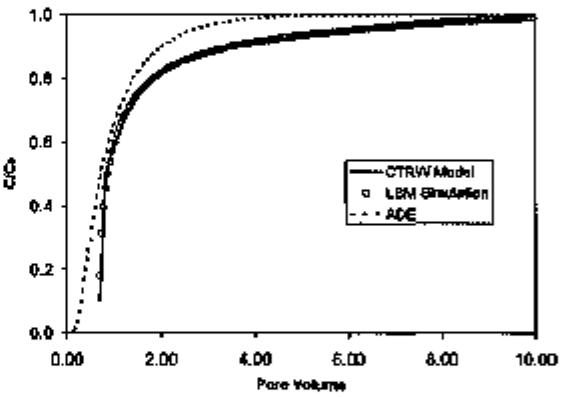

The breakthrough and $\psi(t)$ are plotted against the number of pore volumes eluted. Pore volume refers to the volume of fluid occupying the pore space of a porous medium; for saturated conditions, it is the total volume of a porous medium minus the total volume of solids that comprise the medium.

For a domain with cross-sectional area A and volumetric fluid content θ (equal to 1 for flow in a slit), the number of pore volumes is calculated by dividing the volume of fluid leached through the column ($V = A\theta\bar{u}t$) by the fluid capacity ($V_0 = A\theta L$) of the medium

$$T = \frac{V}{V_0} = \frac{A\theta\bar{u}t}{A\theta L} = \frac{\bar{u}t}{L}. \tag{19}$$

The pore volume is routinely used to non-dimensionalize time in studies of solute breakthrough by dividing the volume of fluid eluted from the medium by one pore volume. This is convenient because it enables rapid comparison to piston flow, where solutes entering the medium at 0 pore volumes would elute when 1 pore volume of solute-laden fluid has passed through the medium. In the macroscopic porous medium LBM application

here, 1 pore volume equals the total volume because the 'solids' that damp the flow occupy 0 volume. Both relative concentration and pore volume are dimensionless, and are used to non-dimensionalize breakthrough curves.

4.2 *Porous medium with conduit at low Re*

As a model of a heterogeneous porous medium traversed by a conduit, we use a randomly generated $81\,lu \times 81\,lu$ domain with a fractal permeability distribution as shown in grey scale in Figure 3. White indicates open pores, black represents solid particles or zero permeability and grey represents intermediate permeability. In this case n_s is strictly less than 1. The fractal domain in grey scale resembles the heterogeneous background of a porous medium.

Figure 3 Heterogeneous fractal domain with curved channel in the middle

We use the probabilistic bounce-back model to simulate flow through the porous domain, and the Navier-Stokes equation is solved in the open conduit/channel (white zone). We studied two different cases depending upon the background heterogeneity. The background could be heterogeneous or homogeneous. For the homogeneous background, n_s is uniformly equal to 0.1.

A constant concentration boundary is enforced at the inlet and a zero concentration gradient boundary is applied at the exit. The domain is periodic transverse to the direction of flow. Flow is pressure driven with a density difference of $10^{-3}\,mu/lu^2$ between the inlet and exit boundaries. Transport is advection dominated; diffusion is kept at a minimum with the relaxation parameter for the solute component set equal to 0.501 ts and the dispersivity ratio (α_L/α_T) is 3. The relaxation parameter τ for the fluid is set to 1.0 ts. In this case, Re = 5.4 in the curved channel and no eddy mixing is expected. We use CTRW to fit the LBM simulations. The $\psi(t)$ function obtained is presented in Figure 4. Unlike the monotonically decreasing $\psi(t)$ obtained for the Poiseuille flow, this curve shows a peak at approximately 1.5 pore volume that corresponds to the onset of solute discharge from the porous background. While the ADE is grossly incapable of fitting the results, breakthrough curves measured at the downstream end of the domain are well-fitted with the CTRW model as shown in Figure 5.

Figure 4 ψ function vs. pore volumes for simulations in domain of Figure (3)

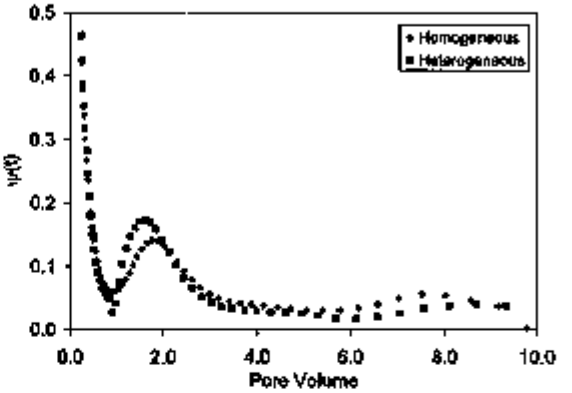

Figure 5 Breakthrough curve at the downstream end of the domain with homogeneous and heterogeneous porous background with a curved conduit in the middle as shown in Figure 3

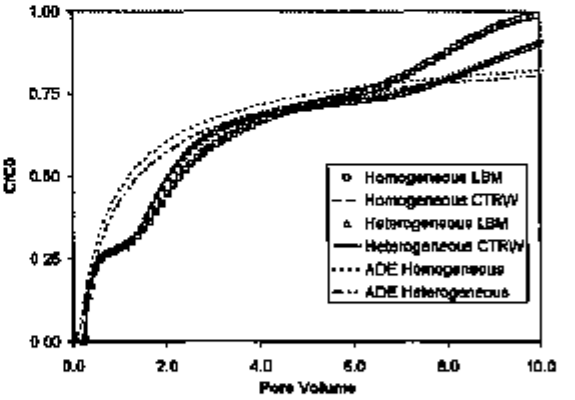

4.3 *Eddy mixing*

Perhaps the simplest flow system that includes the possibility for eddy mixing is flow over a square obstacle. The domain is 400 lu long and 100 lu wide. Flow is gravity driven, with $g = 10^{-7} lu/ts^2$. The relaxation parameter for the fluid is set to 0.51 ts to induce an eddy behind the obstacle. The relaxation parameter for solute is equal to 0.51 ts. Figure 6 shows a recirculating eddy flow at Re = 100 after a square obstruction ($25lu \times 25lu$) in a straight channel.

Figure 7 gives the computed $\psi(t)$ function. It is more akin to the zero-diffusion Poiseuille flow $\psi(t)$ (Fig. 1) than to the $\psi(t)$ for the domain comprised of the porous medium and conduit at low Re (Fig. 4), yet important differences account for transient diffusion into and out of the eddy.

Figure 6 Velocity field showing eddy circulation behind a square obstacle at Re = 100

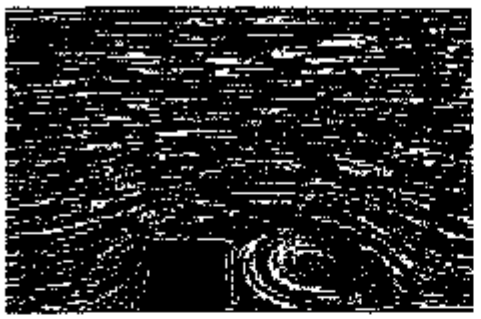

Figure 7 ψ function vs. time for circulating eddy

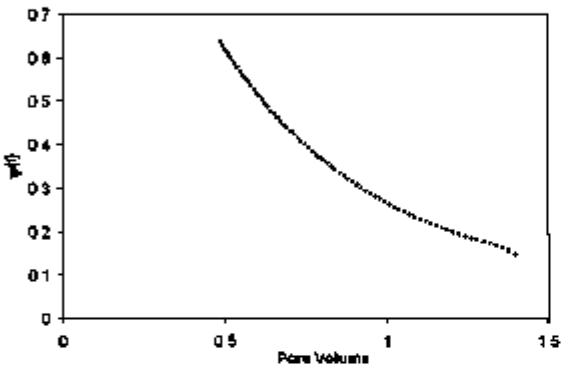

We measured the breakthrough curve at the end of the domain and fitted the ADE and CTRW models as shown in Figure 8.

Figure 8 Breakthrough curve at the end of the domain, for flow as shown in Figure 6

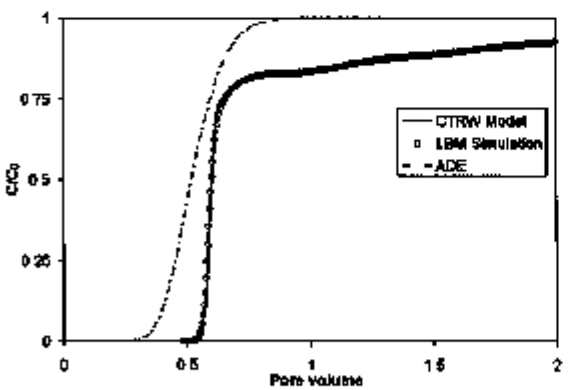

The ADE fails to capture the character of the curve, which exhibits a very sudden rise to approximately 0.8 of full breakthrough followed by a lengthy tailing period due to diffusion into and out of the recirculating eddy. Similar results are expected in more complicated flow systems that involve conduits and eddies.

As a final example, we measured breakthrough curve at the end of the domain for turbulent flow at Re = 900 in a fractal domain (81 lu × 81 lu) with a curved channel (Fig. 9). The flow is gravity driven, $g = 10^{-6} lu/ts^2$. Relaxation parameters for the fluid and solute are 0.501 ts and 0.51 ts respectively. In the porous medium α_L/α_T is again equal to 3. The maximum velocity attained in channel is 0.0535 lu/ts and the characteristic length for Re calculation is the width of the channel at the inlet that is 25 lu.

Figure 9 Fractal domain with curved channel in the middle modified to enhance turbulence

The $\psi(t)$ derived from the LBM simulation (Fig. 10) results is particularly complex. CTRW is again capable of fitting the LB simulation of the complex solute transport process far better than the ADE as shown in Figure 11.

Figure 10 ψ function against pore volume on semi-log scale for simulation in Figure 9

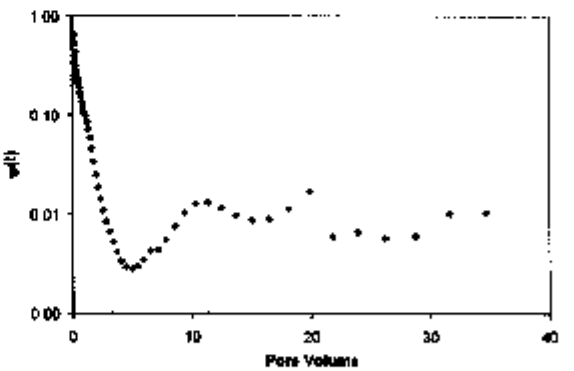

5 Conclusion

These results indicate that CTRW has excellent potential for modelling complex solute transport problems. Using LBM to simulate such solute transport processes may allow linkages between CTRW parameters and porous medium, conduit, and fluid dynamic characteristics to be established. Further analysis of the velocity distributions in the domains and their relationships with the derived $\psi(t)$ functions is necessary. This ultimately may allow CTRW

parameters to be estimated from readily observable porous medium and fluid dynamical properties and applied to challenging field problems

Figure 11 Breakthrough curve at the end of the domain with heterogeneous porous background and a curved conduit in the middle as shown in Figure 9 Flow is turbulent at Re = 900

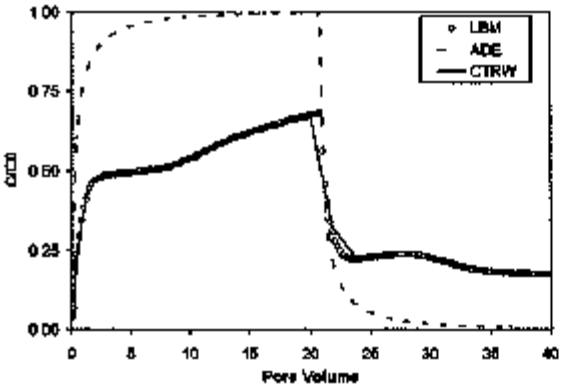

Acknowledgements

The authors are grateful to an anonymous reviewer for expert and insightful suggestions that have improved the quality of this manuscript The authors are thankful to Dr Thorne for technical assistance This work was supported by the National Science Foundation under Grant No EAR 0440253, and by the U S Department of Energy under Contract No DE-AC02-05CH11231

References

Balasubramanium, K , Hayot, F and Saam, W F (1987) 'Darcy's law from lattice-gas hydrodynamics', *Phys Rev E* , Vol 36, No 5, pp 2248–2253

Bear, J (1979) *Hydraulics of Groundwater*, McGraw Hill, New York

Berkowitz, B , Cortis, A , Dentz, A and Scher, H (2006) 'Modeling non-fickian transport in geological formations', *Rev Geophys* , Vol 44, No 2, June, doi 10 1029/2005RG000178

Capuani, F , Frenkel, D and Lowe, C P (2003) 'Velocity fluctuations and dispersion in a simple porous medium', *Phys Rev E* , Vol 67, No 5, pp 056306 1–056306-8

Cortis, A (2007) 'Péclet-dependent memory kernels for transport in heterogeneous media', *Physical Review E*, Vol 76, No 3, pp 030102-1–030102 4

Cortis, A and Berkowitz, B (2004) 'Anomalous transport in 'Classical' soil and sand columns', *Soil Sci Soc Am J* , Vol 68, No 5, pp 1539–1548

Dardis, O and McCloskey, J (1998) 'Lattice Boltzmann scheme with real numbered solid density for the simulation of flow in porous media', *Phys Rev E* , Vol 57, No 4, pp 4834–4837

Field, M S (1993) 'Karst hydrology and chemical contamination', *J Environ Syst* , Vol 22, No 1, pp 1–26

Flekkøy, E G (1993) 'Lattice Bhatnagar Gross Krook models for miscible fluids', *Phys Rev E* , Vol 47, No 6, pp 4247–4257

Freed, D M (1998) 'Lattice Boltzmann methods for macroscopic porous media modeling', *Int J Mod Phys C* , Vol 9, No 8, pp 1491–1503

Freeze, R A and Cherry, J A (1979) *Groundwater*, Prentice-Hall, Englewood Cliffs, NJ, USA

Gao, Y and Sharma, M M (1994) 'A LGA model for fluid flow in heterogeneous porous media', *Transport Porous Med* , Vol 17, No 1, pp 1–17

Ginzburg, I (2005) 'Equilibrium-type and link-type lattice Boltzmann models for generic advection and anisotropic-dispersion equation', *Adv Water Resour* , Vol 28, No 11, pp 1171–1195

Ginzburg, I and d'Humières, D (2003) 'Multi-reflection boundary conditions for lattice Boltzmann models', *Phys Rev E* , Vol 68, pp 066614-1–066614 30

Inamuro, T , Yoshino, M , Inoue, H , Mizuno, R and Ogino, F (2002) 'A lattice Boltzmann method for a binary miscible fluid mixture and its application to a heat-transfer problem', *J Comp Phys* , Vol 179, No 1, pp 201–215

Kang, Q , Zhang, D and Chen, S (2002) 'Unified lattice Boltzmann method for flow in multiscale porous media', *Phys Rev E* , Vol 66, No 5, pp 056307-1–056307-11

Pan, C , Luo, L S and Miller, C T (2006) 'An evaluation of lattice Boltzmann schemes for porous medium flow simulation', *Computers and Fluids*, Vol 35, Nos 8–9, pp 898–909

Qian Y , d'Humières, D and Lallemand, P (1992) 'Lattice BGK models for Navier-Stokes equation', *Europhys Lett* , Vol 17, No 6, pp 479–484

Spaid, M A A and Phelan Jr , F R (1997) 'Lattice Boltzmann methods for modeling microscale flow in fibrous porous media', *Phys Fluids*, Vol 9, No 9, pp 2468–2474

Sukop, M C and Thorne Jr , D T (2006) *Lattice Boltzmann Modeling An Introduction for Geoscientists and Engineers*, Springer, Heidelberg, Berlin, New York

White, W B and White, E L (2005) 'Ground water flux distribution between matrix, fractures, and conduits constraints on modeling', *Speleogenesis and Evolution of Karst Aquifers*, Vol 3, No 2, pp 2–8

Zhang, X , Bengough, A G , Crawford, J W and Young, I M (2002a) 'A lattice BGK model for advection and anisotropic dispersion equation', *Adv Water Resour* , Vol 25, No 1, pp 1–8

Zhang, X , Crawford, J W , Bengough, A G and Young, I M (2002b) 'On boundary conditions in the lattice Boltzmann model for advection and anisotropic dispersion equation', *Adv Water Resour* , Vol 25, No 6, pp 601–609

Zou, Q and He, X (1997) 'On pressure and velocity boundary conditions for the lattice Boltzmann BGK model', *Phys Fluids*, Vol 9, No 6, pp 1591–1598